One-proton breakup of ^{24}Si and the ^{23}Al(p,γ)^{24}Si reaction in type I x-ray bursts

A. Banu, F. Carstoiu, N. L. Achouri, W. N. Catford, M. Chartier, B. Fernández-Domínguez,
M. Horoi, B. Laurent, N. A. Orr, S. Paschalis, N. Patterson, B. Pietras, B. T. Roeder, P.
Roussel-Chomaz, J. S. Thomas, L. Trache, and R. E. Tribble

One-proton breakup of ^{24}Si and the ^{23}Al$(p,\gamma)^{24}$Si reaction in type I X-ray bursts

A. Banu,[1, *] F. Carstoiu,[2] N. L. Achouri,[3] W. N. Catford,[4] M. Chartier,[5] B. Fernández-Domínguez,[5, †]
M. Horoi,[6] B. Laurent,[3, ‡] N. A. Orr,[3] S. Paschalis,[5, §] N. Patterson,[4] B. Pietras,[5, †] B.
T. Roeder,[7] P. Roussel-Chomaz,[8, ¶] J. S. Thomas,[4, **] L. Trache,[7] and R. E. Tribble[7]

[1]*Department of Physics and Astronomy, James Madison University, Harrisonburg, VA 22807, USA*
[2]*National Institute of Physics and Nuclear Engineering "Horia Hulubei" (IFIN-HH), R-077125 Magurele-Bucharest, Romania*
[3]*LPC-ENSICAEN, IN2P3-CNRS et Université de Caen, 14050 Caen Cedex, France*
[4]*Department of Physics, University of Surrey, Guildford GU2 5XH, UK*
[5]*Oliver Lodge Laboratory, University of Liverpool, Liverpool L69 7ZE, UK*
[6]*Department of Physics, Central Michigan University, Mount Pleasant, Michigan 48859, USA*
[7]*Cyclotron Institute, Texas A&M University, College Station, TX 77843, USA*
[8]*Grand Accélérateur d'Ions Lourds, BP 55027, 14076 Caen Cedex 5, France*
(Dated: June 26, 2012)

Background: To understand explosive hydrogen burning in stars and to explore various explosive scenarios such as type I X-ray bursts (XRBs), reliable reaction rates are needed. The cross sections for radiative proton capture on near-dripline nuclei are necessary for the determination of the reaction rates, but cannot be measured directly.

Purpose: To determine the reaction rate for the radiative proton capture reaction ^{23}Al(p,γ)^{24}Si using indirect methods and, as a consequence, evaluate if sequential 2p capture on ^{22}Mg seed nuclei is significant at high temperatures.

Method: Nonresonant radiative proton capture on ^{23}Al is investigated using the one-proton breakup of ^{24}Si at 61 MeV/nucleon and the asymptotic normalization coefficient (ANC) for ^{24}Si$_{gs} \rightarrow$ ^{23}Al $+ p$ is deduced.

Results: From the ANC, the nonresonant component of the astrophysical S-factor for the ^{23}Al(p,γ)^{24}Si reaction is determined and, using other new experimental data the resonant component is re-evaluated.

Conclusions: The ^{23}Al(p,γ)^{24}Si reaction is of interest for type I XRB nucleosynthesis and its reaction rate can affect both the ^{22}Na abundance and the total energy output. New determinations of the rates for the ^{22}Mg(p,γ)^{23}Al(p,γ)^{24}Si reaction chain are provided here and we point to the need that they be included in XRB scenarios.

PACS numbers: 21.10.Jx, 25.60.Gc, 26.30.Ca, 27.30.+t

* banula@jmu.edu
† Present address: Universidade de Santiago de Compostela, E-15706 Santiago de Compostela, Spain
‡ Present address: CEA, DAM, DIF, F-91297 Arpajon Cedex, France
§ Present address: Techniche Universität Darmstadt, Institut für Kernphysik, Schlossgartenstraße, 64289 Darmstadt, Germany
¶ Present address: DSM/Dir CEA Saclay, F-91191, Gif-sur-Yvette, France
** Present address: School of Physics and Astronomy, The University of Manchester, Manchester M13 9PL, UK

I. INTRODUCTION

Owing to their short recurrence period (hours to days), type I X-ray bursts (XRBs) constitute the most frequent type of thermonuclear stellar explosion in the Galaxy, with about 100 sources known so far, and the third in terms of total energy output after supernovae and classical novae, with an energy release of about 10^{39} - 10^{40} erg in 10 - 100 s. It is thought that XRBs occur in binary star systems, where a neutron star accretes matter from its companion, a main sequence star [1]. As the accreted hydrogen- and helium-rich matter builds up on the surface of the neutron star, the temperature and pressure increase and a thermonuclear runaway (reaching peak temperatures of $T = 1$-2 GK) occurs, which is observed as an X-ray burst. The fact that these bursts do not destroy the binary star system makes X-ray binaries useful to study matter under extreme temperature and density conditions.

The XRBs are characterized by ignition driven by the ^{4}He($\alpha\alpha,\gamma$)^{12}C reaction and rapid breakout from the hot CNO cycles, followed by helium burning via the (α,p)-process and hydrogen burning via the rp-process [2]. The nuclear reaction flows can be temporarily stalled at so-called *waiting-point* nuclei which are characterized by β^+-decay half-lives on the order of seconds (significantly long on the XRB time scale) and by very low proton capture Q-values. This hampers further proton capture since the captured proton is easily removed by photodisintegration at the very high temperatures of XRBs or by proton decay. But other processes, such as β^+-decay or (α,p) reactions, could also occur. The question then is, whether proton capture still plays a role or β^+-decay and (α,p) reactions indeed dominate the destruction of the waiting-point nuclei. This is an important issue as the composition of the rp-process ashes determines the composition of the crust forming the surface of the neutron star. For a given initial composition, it is the endpoint of the (α,p)-process (up to $A = 41$) that determines the heaviest nuclei that would be produced by the rp-process in consuming all of the hydrogen [3]. However, in X-ray bursts the rp-process might not reach these nuclei, since the burning time is limited to the burst timescale (~ 100 s). To understand the accretion rate dependence of the final isotopic composition reliable reaction rates for both the (α,p) reactions and proton capture on the waiting-point nuclei are required. Specifically in the mass region $A = 20$-40, the β^+-unstable even-even $T_z = (N - Z)/2 = $ -1 isotopes, ^{22}Mg, ^{26}Si, ^{30}S, and ^{34}Ar, are potential waiting points of importance as most of the reaction flow passes through them [4]. For these nuclei the individual reaction rates determine whether β^+-decay, the (α,p) reaction or proton capture dominates.

In this work we focus on the case of ^{22}Mg as a potential waiting point where proton capture competes with the (α,p) reaction. Owing to the small Q-value (141.11(43) keV [5]), the ^{22}Mg(p,γ)^{23}Al reaction is in thermal equilibrium with the inverse reaction ^{23}Al(γ,p)^{22}Mg at X-ray burst temperatures and densities. Break out from the (p,γ)(γ,p)-equilibrium requires a high ^{23}Al(p,γ)^{24}Si reaction rate. The influence of (sequential) two-proton capture on ^{22}Mg forming ^{24}Si via ^{22}Mg(p,γ)^{23}Al(p,γ)^{24}Si, which becomes important at higher temperatures, is of interest here. The 2p-capture rate on ^{22}Mg depends only on the proton separation energy of ^{23}Al, which fixes the equilibrium ^{23}Al abundance, and the ^{23}Al(p,γ)^{24}Si reaction rate. This reaction occurs via nonresonant (direct) and/or resonant radiative capture. Previously, Schatz *et al.* [6] evaluated the resonant contributions and used shell-model predictions from Herndl *et al.* [7] to determine the nonresonant contribution.

Here we employ indirect techniques [8, 9] to evaluate the ^{23}Al(p,γ)^{24}Si reaction rate. Specifically, the cross section and momentum distribution of ^{23}Al fragments from the one-proton breakup of ^{24}Si were measured and compared to Glauber-type calculations. This enabled us to deduce the corresponding spectroscopic factor and to determine for the first time the asymptotic normalization coefficient (ANC) for ^{24}Si$\rightarrow^{23}$Al $+ p$. The ANC was then employed to evaluate the *nonresonant* component of the astrophysical S-factor for ^{23}Al(p,γ)^{24}Si. In addition, a revised calculation of the *total* reaction rate was made by taking into account a recent high-precision mass measurement of ^{23}Al [5], which has implications on the resonant energies in ^{24}Si as well as on the uncertainty of the *resonant* reaction rate.

II. EXPERIMENT

A cocktail of proton-rich nuclei as secondary beams was obtained by fragmentation of a 95 MeV/nucleon ^{32}S primary beam, provided by the Coupled Cyclotron Facility at GANIL, impinging on a carbon target. A secondary carbon target, 175 mg/cm^2 thick, was placed at the target of the SPEG spectrograph [10] which was employed to measure the momentum distributions of the breakup fragments. SPEG was operated at 0° in an achromatic mode on target, whereby an intrinsic resolution of δp/p $\sim 5\times10^{-4}$ (FWHM) was achieved. The final momentum resolution, including the secondary beam energy spread and target effects, was δp/p $\sim 5\times10^{-3}$ (FWHM). The large angular acceptance of the spectrometer (4° in the horizontal and vertical planes) provided for complete collection of the breakup fragments, obviating any ambiguities in the integrated cross sections and longitudinal momentum distributions. Event-by-event particle identification was performed with the SPEG focal-plane detection system consisting of a gas ionization chamber to measure the energy loss (ΔE), two large-area drift chambers to reconstruct focal-plane position, and a thick plastic scintillator in which the secondary beam was stopped and the residual energy (E) determined. The time-

of-flight was measured using the timing information provided by this plastic detector and the cyclotron radio frequency. The momenta of the breakup fragments relative to the incident projectiles in the laboratory frame were transformed into that in the projectile rest frame using Lorentz transformation. To compare the measured distributions with the theoretical ones, all broadening effects inherent in the measurements have been taken into account through Monte Carlo simulations. These effects include the energy spread in the beam, the differential energy losses of the projectile and the fragment in the target, the energy and angular straggling in the target, and the detector and spectrometer resolutions. The secondary carbon target was surrounded by a γ-ray detection system consisting of 8 EXOGAM Germanium detectors [11] and 12 NaI detectors. In the data analysis for the ^{24}Si one-proton breakup case, the γ-ray information is not relevant, as will be discussed later in the paper. Hence, we skip here experimental details about the γ-ray detection system and γ-ray data analysis, which, however, are to be found in our previous work [8].

By knowing the value of the primary beam intensity, the intensities of the secondary beam ions were derived from several empty-target normalization runs made with SPEG set to the same magnetic rigidity as the beam line. Based on the fluctuations between the different runs a normalization uncertainty of 11% was estimated. Among the fourteen ion species of the secondary cocktail beam plotted in Fig. 1, the ^{24}Si projectiles had an average intensity of about 30 particles per second and an energy of 61 MeV/nucleon.
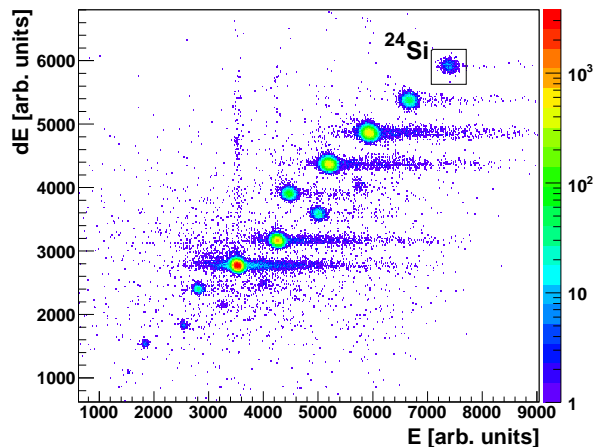

FIG. 1. (Color online) Particle identification of the secondary cocktail beam plotted as energy loss in the ionization chamber versus residual energy in the thick plastic detector.

III. RESULTS AND DISCUSSION

To describe the nuclear component of the one-proton breakup (the dominant mechanism for a carbon target), an extended version of the Glauber model, which incorporates second-order non-eikonal corrections in the evaluation of the scattering amplitude that defines the stripping and diffraction transition operators, has been employed. The formalism used is presented in Ref. [12].

The one-proton removal cross sections are calculated as an incoherent sum of single-particle configurations,

$$\sigma_{-1p}^{th} = \sum SF(c; nlj)(\sigma_{sp}^{stripp}(nlj) + \sigma_{sp}^{diff}(nlj) + \sigma_{sp}^{C}(nlj)), \tag{1}$$

where the sum extends over the single-particle quantum numbers nlj of the orbital coupled to a given core state c, SF are the spectroscopic factors, while σ_{sp}^{stripp} is the single-particle stripping cross section, σ_{sp}^{diff} is the single-particle diffractive breakup cross section, and σ_{sp}^{C} is the Coulomb dissociation cross section. We employ the nucleon-nucleon effective interaction of Jeukenne, Lejeune and Mahaux (JLM) [13] to evaluate the optical potentials for the proton-target and core-target systems using the double-folding procedure established in [14, 15], while the Coulomb dissociation is treated within first-order perturbation theory, including final-state interactions. For the proton-target system, we normalized the JLM folding potentials used in the second order eikonal approximation to the global Dirac phenomenology from Ref. [16]. The single-particle densities for the core of the projectile and target used here were obtained from a standard spherical HF + BCS calculation using the density functional of Beiner and Lombard [17], and adjusted to reproduce total binding energy. The root-mean-square (rms) charge radius obtained in this calculation for the ^{23}Al core is $< r_{ch}^2 >^{1/2} = 3.14$ fm, which compares well with the experimental value for ^{27}Al (3.06±0.09 fm)

[18]. The calculated rms charge radius of the ^{12}C target is almost identical with the experimental value (2.472 ± 0.015 fm) [18].

The low-lying nuclear structure of ^{24}Si can be assumed to be that of a core plus a valence proton ($^{23}Al + p$). Because there are no known particle-bound excited states in ^{23}Al, the ^{24}Si $J^\pi = 0^+$ ground-state wave function will only have a single configuration that couples a proton to the core ground state, $^{23}Al(5/2^+)_{gs} \otimes \pi 1d_{5/2}$, which is the configuration of astrophysical interest for the nonresonant (direct) radiative capture ^{23}Al(p,γ)^{24}Si. Hence, no γ rays would be expected in coincidence with the measured ^{23}Al residues, and indeed, in the Doppler corrected γ-ray energy spectra none were observed. Other possible components of the ground state, such as $^{22}Mg(0^+)_{gs} \otimes [\pi 2s_{1/2}]^2_{0^+}$ or $^{22}Mg(0^+)_{gs} \otimes [\pi 1d_{3/2}]^2_{0^+}$, will lead to unbound ^{23}Al* states, and will, therefore, contribute to the $^{22}Mg + 2p$ final channel, which was clearly observed in our experiment via particle-gamma coincidences correlating the ^{24}Si projectiles and the ^{22}Mg breakup residues detected in SPEG [8].

To generate the $1d_{5/2}$ wave functions of the valence proton, a spherical Woods-Saxon (WS) potential was chosen. The depth of the central bound-state potential was adjusted to reproduce the experimental proton binding energy in ^{24}Si ($S_{1p} = 3.30$ MeV). The spin-orbit component was taken in the Thomas form with a standard strength, while the Coulomb component was generated by a uniform charge distribution with a radius equal to the nuclear value. Calculations of total single-particle breakup cross sections were performed for a series of central Woods-Saxon potentials for which both geometrical parameters (R_0,a) - nuclear radius and diffuseness - were varied in steps of 0.02 fm from $R_0 = 3.30$ to 3.46 fm such as that for each R_0 the difuseness had values from $a = 0.50$ fm to 0.66 fm. Moreover, to take into account the effect of the projectile energy loss in the target, the cross sections were calculated at energies of 61, 53, and 45 MeV/nucleon, corresponding to the breakup occuring at the front, the middle and the back of the target, respectively.

A. Asymptotic normalization coefficient for $^{24}Si_{gs} \to^{23} Al + p$

In nuclear astrophysics studies of radiative capture reactions, an essential quantity of interest is the large-distance behavior of the bound-state wave function. At large distances from the nucleus, the radial form of the tail of the bound-state wave function is determined by the Whittaker function, which is regular at infinity[19].

The basis of the ANC determination for the ^{23}Al(p,γ)^{24}Si reaction rate is that the cross section for this *peripheral* reaction is determined by the square of the ANC for ^{24}Si $\to$ ^{23}Al + p. In our case, the ANC is the amplitude of the tail of the projection of the bound-state wave function of ^{24}Si on the two-body channel ^{23}Al + p.

For the peripheral one-proton breakup of ^{24}Si, the following relationship is applicable between the spectroscopic factor and the asymptotic normalization coefficient (ANC) that characterize the removed proton in the ground-state wave function of ^{24}Si,

$$SF(c; nlj) = C^2(c; nlj)/b^2_{sp}(nlj), \tag{2}$$

where $C(c; nlj)$ and b_{sp} are the ANC of the system $^{24}Si \to$ $^{23}Al + p$ and the single-particle ANC, respectively. By comparing the integral experimental cross section to the theoretical single-particle breakup cross section, an experimental spectroscopic factor, SF_{exp}, may be deduced from the relationship

$$SF_{exp} = \sigma_{exp}/\sigma^{th}_{sp}. \tag{3}$$

From Eqs. (1), (2) and (3), an expression is obtained for the square of the asymptotic normalization coefficient for a given l, as follows

$$C^2_l = \frac{\sigma_{exp}}{\sigma^{th}_{sp}} \left(\frac{r_L R_l(r_L)}{W_{-\eta,l+1/2}(2\kappa r_L)} \right)^2, \tag{4}$$

where R_l is the normalized radial wave function, r_L is an asymptotic distance, W is the Whittaker function with the Sommerfeld parameter η and the bound-state wave number κ, while the term within the parantheses is the single-particle ANC. This expression illustrates how in the case of peripheral reactions the asymptotic normalization coefficient can be obtained more accurately, or rather, in a manner which is less dependent on the parameters used for the proton binding potential, than the spectroscopic factor. The essential point is that the calculated cross section is directly proportional to the asymptotic part of the radial overlap integral, which is uniquely defined by the ANC. In Fig. 2 we compare the ANC squared for $^{24}Si_{gs} \to$ ^{23}Al + p and the experimental spectroscopic factor as a function of the single-particle ANC, for several of the Woods-Saxon potential geometries mentioned before in the section. The spectroscopic factor depends rather strongly on the choice of the geometry of the proton binding potential ($\sim 36\%$ variation), while the ANC squared has a weaker, though not insignifiant, dependence ($\sim 27\%$ variation). This is due
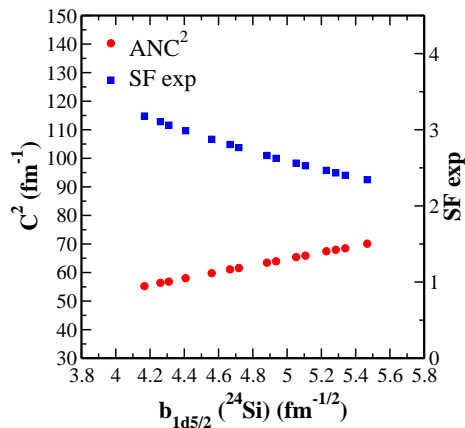
FIG. 2. (Color online) Dependence of the ANC squared and of the experimental spectroscopic factor, for the ground state of ^{24}Si, on the single-particle ANC, $b_{1d_{5/2}}$.

TABLE I. Experimental cross section, calculated (see text) single-particle breakup cross sections (total, stripping, nuclear diffraction, Coulomb dissociation), and the corresponding experimental spectroscopic factor and the ANC. The uncertainties in the calculations arise from the uncertainties in the geometry of the Woods-Saxon binding potential, the effect of energy loss in the target, and the uncertainties in the normalization of the the proton-target and core-target JLM optical potentials.

σ_{exp} [mb]	σ_{sp}^{th} [mb]	σ_{sp}^{stripp} [mb]	σ_{sp}^{diff} [mb]	σ_{sp}^{Coul} [mb]	SF_{exp}	$C_{1d_{5/2}}^2$ [fm^{-1}]
61(7)	23(2)	14(1)	8(1)	0.8(1)	2.7(2)	62(4)

to the fact that ^{24}Si is a relatively well-bound nucleus ($S_{1p} = 3.30$ MeV).

Depending on the aforementioned geometries of the central Woods-Saxon potential that were considered, we obtained a range of values for the ANC and the corresponding spectroscopic factor. In all cases, to assess quantitatively the agreement between the measured longitudinal momentum distributions and the theoretical differential cross sections, standard χ^2 (chi square) values were computed taking into account the experimental statistical uncertanties. Weighted average values were obtained for the stripping, diffraction, Coulomb dissociation and the total single-particle cross section, with inverse of the reduced chi-square values taken as weights. These results are presented in Table I along with the experimental cross section and the corresponding weighted average values of the experimental spectroscopic factor and the asymptotic normalization coefficient.

The experimental value of 61(7) mb for the breakup cross section takes into account a correction of $\sim 4\%$ applied for missing events in the low momentum region of the momentum distribution. To estimate the experimental uncertainty, the normalization uncertainty of 11% was added in quadrature with the target thickness uncertainty of 3%. We determined the ANC squared of interest here to be $C_{d_{5/2}}^2(^{24}Si_{gs}) = 62(8)$ fm^{-1}. The uncertainty also takes into account the uncertainties in the geometry of the Woods-Saxon potential, the effect of energy loss in the target, and the uncertainties in the JLM optical potentials.

The measured momentum distribution in the ^{23}Al reference frame is plotted in Fig. 3 along with momentum distributions calculated in the extended Glauber model for the $[^{23}Al(5/2^+)_{gs} \otimes \pi 1d_{5/2}]_{0^+}$ configuration of the ^{24}Si ground state. The upper and lower limits (shaded area) of the theoretical momentum distribution illustrate the combined effects of uncertainty in the geometry of the proton-binding Woods-Saxon potential, energy loss in the target, and uncertainty in the normalization of the JLM optical potentials. *The central theoretical curve (plotted by weighting the single-particle differential cross section with the weighted average value of 2.7(2) obtained for the experimental spectroscopic factor) corresponds to calculations for which a Woods-Saxon potential with a nuclear radius and diffuseness, $R_0 = 3.38$ fm and $a = 0.60$ fm, respectively, was chosen.* We underline that the values obtained for the stripping, diffraction, and Coulomb dissociation components of the total single-particle breakup cross section agree reasonably well with the corresponding weighted average values presented in Table I. Therefore, it was this Woods-Saxon potential that was used to calculate the astrophysical S-factor for the direct radiative capture ^{23}Al(p,γ)^{24}Si, as will be discussed in the following subsection.

Fig. 4 shows the stripping and diffractive breakup probabilities as a function of the length of the projection of the proton-core radius on a plane perpendicular to the direction of motion of the projectile (this is to a good approximation equivalent with the proton-core radial distance). For the single-particle breakup cross section calcula-
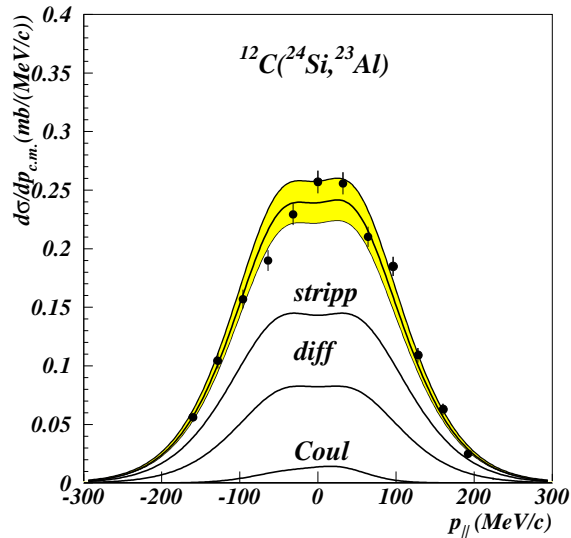
FIG. 3. (Color online) Experimental momentum distribution of the ^{23}Al breakup fragments (points) compared with a theoretical distribution calculated (see text) for the $[^{23}Al(5/2^+)_{gs} \otimes \pi 1d_{5/2}]_{0^+}$ configuration of the ^{24}Si ground state.
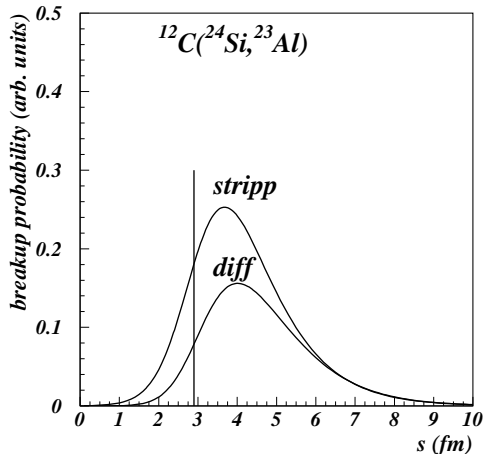

FIG. 4. Breakup probabilities as a function of proton-core impact parameter. The vertical line denotes the Hartree-Fock core *rms* radius. The internal region contributes some 12 % to the total breakup probability.

tions, the aforementioned Woods-Saxon potential ($R_0 = 3.38$ fm and $a = 0.60$ fm) was chosen to generate the $1d_{5/2}$ single-particle wave functions. We estimated that the internal region contributes only some 12% to the total reaction probability, demonstrating the rather peripheral character of the reaction. (Most of this contribution arises from the increased refractive power of the proton-target optical potential as compared to core-target optical potential.)

As noted above, for the experimental spectroscopic factor, we obtained a value of 2.7(2) whereas large-scale shell model calculations based on the USDB effetive interaction [20] predict the ground-state spectroscopic factor of ^{24}Si to be $SF(5/2^+) = 3.42$. With a center-of-mass correction applied $\left(\left(\frac{A}{A-1}\right)^2\right)$ and taking into account the value of the theoretical single-particle breakup cross section of 23(2) mb (see Table I), this yields a total theoretical breakup cross section of $\sigma_{total}^{th} = 85.1$ mb. Hence, a reduction factor [21], $R_s = \sigma_{exp}/\sigma_{total}^{th}$, of 0.72(10) is obtained, which agrees well with that of 0.79(4) from Ref. [22] for the ^{9}Be(^{24}Si,^{23}Al)X reaction at 85.3 MeV/nucleon. However, we cannot conclude that is a reduction of the spectroscopic factor but rather a reduction of the experimental cross section

TABLE II. ^{23}Al(p,γ)^{24}Si: nonresonant capture transitions and the astrophysical S-factors, $S(E_0)$, where E_0 is the effective mean energy for the radiative capture at a temperature of 1 GK, E^* are the excitation energies of the bound states in ^{24}Si, l_i the orbital angular momentum of the incoming proton, $(nl_j)_f$ and SF_f are the quantum numbers and spectroscopic factors, respectively, corresponding to the proton-bound final states in ^{24}Si. The spectroscopic factors corresponding to the configurations of ^{24}Si(2_1^+) are from a large-scale shell model calculation using the USDB effective interaction [20].

E^* (MeV)	J^π	l_i	$(nl_j)_f$	SF_f	$S(E_0)$ (MeVb) at $T_9 = 1$ GK
0.000	0_1^+	p, f	$1d_{5/2}$	2.7(2) (this work)	0.99×10^{-3}
1.879	2_1^+	p, f	$2s_{1/2}$	0.251 (shell model)	1.89×10^{-3}
		p, f	$1d_{3/2}$	0.032 (shell model)	2.92×10^{-5}
		p, f	$1d_{5/2}$	0.177 (shell model)	1.72×10^{-4}

relative to the one evaluated using the shell-model spectroscopic factor and the single-particle breakup cross section.

B. Total reaction rate and nonresonant component of the astrophysical S-factor for ^{23}Al(p,γ)^{24}Si

The radiative proton capture reaction, ^{23}Al(p,γ)^{24}Si, is characterized by a relatively small Q-value of 3.30 MeV, and therefore the reaction rate is determined by single resonances and nonresonant (direct) reaction contributions. The first improved estimate of the reaction rate and of the astrophysical S-factor was made in Ref. [7], where detailed shell-model calculations were performed to compute single-particle spectroscopic factors, excitation energies, as well as γ-ray transition strengths. The calculations showed that the only relevant contribution to the total reaction rate is given by the resonant proton capture via the 2_2^+ state at 3.63 MeV in ^{24}Si. However, the measurement of the excitation energies in ^{24}Si [6] revealed significant deviations from the shell model predictions and allowed for the first time the calculation of the *resonant* contribution of the ^{23}Al(p,γ)^{24}Si reaction rate on the basis of experimental data. Our present results improve further the estimation of the *nonresonant* contribution to the reaction rate over the shell-model based study, by providing for the first time an experimental determination of the spectroscopic factor. In addition, we also update the *total* reaction rate by taking into account new shell model calculations and the recent high-precision mass measurement of ^{23}Al [5] which defines precisely the resonant energies in ^{24}Si, and hence, through the exponential dependence, reduces the uncertainty on the *resonant* reaction rate.

We consider here the capture to the ground state (0^+) and to the first excited state (2_1^+) in ^{24}Si, which are the only *proton-bound* states. The gamma-ray transitions are dominated by the $E1$ multipolarity and by incoming p and f waves. The direct (nonresonant) capture to ^{24}Si ground state involves the proton $1d_{5/2}$ orbital in the final bound state whereas for the direct radiative capture to the 2_1^+ excited state the proton can occupy either the $1d_{5/2}$, $2s_{1/2}$ or $1d_{3/2}$ orbitals. The direct transitions to the ground state and the first excited state have been calculated with the one-body potential model code RADCAP [23]. The calculations were based on the Woods-Saxon potential described earlier ($R_0 = 3.38$ fm and $a = 0.60$ fm). The depths of the potential were adjusted to reproduce the proton binding energy in the ^{24}Si ground state and first excited state ($E^* = 1.879$ MeV). The obtained S-factors corresponding to a temperature of 1 GK are listed in Table II.

The nonresonant reaction rate is calculated in terms of the astrophysical S-factor, $S(E_0)$, in the energy range of the Gamow window relevant for type I X-ray bursts with $T = 0.5$ - 3 GK as in Ref. [24]:

$$N_A \langle \sigma v \rangle_{nr} = 7.83 \times 10^9 \left(\frac{Z}{AT_9^2} \right)^{1/3} S(E_0)[MeVb] exp\left(-4.29 \left[\frac{Z^2 A}{T_9} \right]^{1/3} \right) cm^3 s^{-1} mol^{-1}, \tag{5}$$

where Z is the atomic number of the target nucleus and the reduced mass A is given by $A_p A_T/(A_p + A_T)$ with A_p the projectile mass and A_T the target mass. Here E_0 denotes the effective mean energy for thermonuclear fusion reactions at a given temperature T, and the $S(E_0)$ value of the astrophysical S-factor represents the cumulative yield corresponding to direct (nonresonant) captures to the ground state and the first excited state in ^{24}Si. A reliable calculation of the resonant reaction rates is strongly handicapped by the large uncertainties in the resonance energies, typically 100-150 keV for sd-shell nuclei, which is amplified by the exponential dependence of the reaction rates on the temperature. The authors of Ref. [6] have greatly reduced the uncertainty in the energy of the dominant resonance in the ^{23}Al(p,γ)^{24}Si reaction (corresponding to the second excited state in ^{24}Si) by measuring a resonance energy of 141(31) keV (compared to 320 keV as predicted by the shell model [7]), with the uncertainty dominated by the 25 keV uncertainty in the ^{23}Al mass. Meanwhile, the level of accuracy in the energy of the dominant resonance in the ^{23}Al(p,γ)^{24}Si reaction has been further improved with a recent high-precision mass measurement of ^{23}Al [5]. The
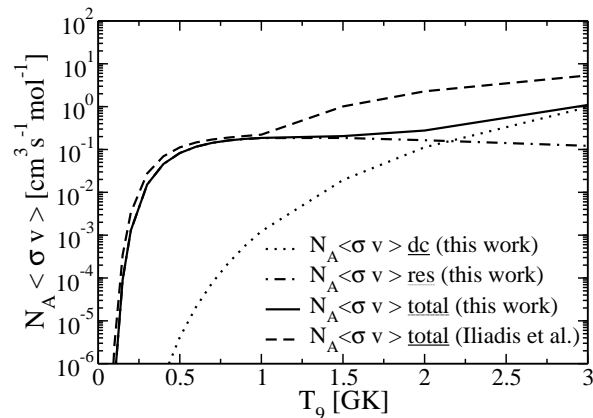
FIG. 5. The total reaction rate for ^{23}Al(p,γ)^{24}Si taking into account the results of the present work for both the direct(nonresonant) and resonant contributions. See text for details.

new value that we determined for the energy of the resonance corresponding to the 2_2^+ excited state in ^{24}Si is $E_{res} = 159(22)$ keV. Based on this value we have recalculated the resonant contribution to the reaction rate [25]:

$$N_A\langle\sigma v\rangle_r = 1.54 \times 10^{11}(AT_9)^{-3/2}\omega\gamma[MeV]exp\left(\frac{-11.605E_r[MeV]}{T_9}\right)cm^3s^{-1}mol^{-1}, \tag{6}$$

where $\omega\gamma = 7.12 \times 10^{-12}$ MeV is taken from Ref. [6].

Our results for the *total* rate of the ^{23}Al(p,γ)^{24}Si reaction are presented in Fig. 5 and Table III in comparison with the recommended reaction rate from the recent compilation of proton capture rates on unstable nuclei in the $A = 20$-40 mass range [26].

IV. CONCLUSIONS

In this work, the radiative proton capture reaction ^{23}Al(p,γ)^{24}Si was investigated indirectly via the one-proton breakup of ^{24}Si at intermediate energies. The asymptotic normalization coefficient (ANC) for the virtual synthesis ^{23}Al + $p \rightarrow$ ^{24}Si was determined for the first time, and a value of $C_{d_{5/2}}^2(^{24}Si_{gs}) = 62(8)$ fm^{-1} was obtained. The corresponding experimental spectroscopic factor, characterizing the $[^{23}Al(5/2^+)_{gs} \otimes \pi 1d_{5/2}]_{0^+}$ configuration of the ^{24}Si ground state, was deduced to be 2.7(2). This enabled us to compute the direct (nonresonant) component of the astrophysical S-factor and the nonresonant reaction rate. We have also revised the resonant contribution to the reaction rate by taking into account the latest high-precision mass measurement for ^{23}Al.

Recently, the authors of Ref. [27] found that the ^{23}Al(p,γ)^{24}Si reaction rate can affect both the ^{22}Na abundance and the total energy output in X-ray bursts. Therefore new hydrodynamical calculations should include the revised reaction rate computed here. Moreover, future experimental work should be undertaken to determine more accurately all the resonance energies in ^{24}Si. In addition, the two "branching" reaction paths at the waiting-point isotope ^{22}Mg - ^{22}Mg(p,γ)^{23}Al(p,γ)^{24}Si and ^{22}Mg(α,p)^{25}Al - compete with each other at high temperature and density conditions of X-ray bursts. As such, the ^{22}Mg(α,p)^{25}Al reaction rate should also be precisely determined.

Finally, as noted in our earlier work [8], the applicability of the technique of ANC determination from one-proton breakup at intermediate energies to investigate proton capture reactions of astrophysical relevance that cannot be measured directly or by other indirect methods has been demonstrated.

TABLE III. Direct(nonresonant), resonant, and total reaction rates for ^{23}Al(p,γ)^{24}Si based on the present work. The last column is the recommended total reaction rate from the recent compilation of Ref. [26].

T^9 (GK)	$N_A \langle \sigma v \rangle_{nr}$ (cm^3 mol^{-1} s^{-1})	$N_A \langle \sigma v \rangle_{res}$ (cm^3 mol^{-1} s^{-1})	$N_A \langle \sigma v \rangle_{total}$ (cm^3 mol^{-1} s^{-1})	$N_A \langle \sigma v \rangle_{Iliadis(2001)}$ (cm^3 mol^{-1} s^{-1})
0.01	7.4×10^{-39}	8.5×10^{-78}	7.4×10^{-39}	3.98×10^{-38}
0.015	5.2×10^{-33}	2.4×10^{-51}	5.2×10^{-33}	2.41×10^{-32}
0.02	2.5×10^{-29}	3.5×10^{-38}	2.5×10^{-29}	1.06×10^{-28}
0.03	1.0×10^{-24}	4.4×10^{-25}	1.5×10^{-24}	5.96×10^{-22}
0.04	8.4×10^{-22}	1.4×10^{-18}	1.4×10^{-18}	2.92×10^{-16}
0.05	9.7×10^{-20}	9.8×10^{-15}	9.8×10^{-15}	7.03×10^{-13}
0.06	3.7×10^{-18}	3.5×10^{-12}	3.5×10^{-12}	1.20×10^{-10}
0.07	6.6×10^{-17}	2.2×10^{-10}	2.3×10^{-10}	4.57×10^{-09}
0.08	7.1×10^{-16}	5.0×10^{-09}	5.0×10^{-09}	6.81×10^{-08}
0.09	5.3×10^{-15}	5.4×10^{-08}	5.4×10^{-08}	5.45×10^{-07}
0.1	3.0×10^{-14}	3.6×10^{-07}	3.6×10^{-07}	2.83×10^{-06}
0.15	1.4×10^{-11}	9.1×10^{-05}	9.1×10^{-05}	3.46×10^{-04}
0.2	6.3×10^{-10}	1.3×10^{-03}	1.3×10^{-03}	3.37×10^{-03}
0.3	7.6×10^{-08}	1.5×10^{-02}	1.5×10^{-02}	2.75×10^{-02}
0.4	1.5×10^{-06}	4.6×10^{-02}	4.6×10^{-02}	6.93×10^{-02}
0.5	1.3×10^{-05}	8.3×10^{-02}	8.3×10^{-02}	1.12×10^{-01}
0.6	6.6×10^{-05}	1.2×10^{-01}	1.2×10^{-01}	1.46×10^{-01}
0.7	2.4×10^{-04}	1.4×10^{-01}	1.4×10^{-01}	1.71×10^{-01}
0.8	7.0×10^{-04}	1.6×10^{-01}	1.6×10^{-01}	1.90×10^{-01}
0.9	1.7×10^{-03}	1.8×10^{-01}	1.8×10^{-01}	2.06×10^{-01}
1.0	3.7×10^{-03}	1.8×10^{-01}	1.9×10^{-01}	2.22×10^{-01}
1.5	5.7×10^{-02}	1.9×10^{-01}	2.4×10^{-01}	$1.01 \times 10^{+00}$
2.0	3.2×10^{-01}	1.6×10^{-01}	4.8×10^{-01}	$2.28 \times 10^{+00}$
3.0	2.9×10^{-01}	1.2×10^{-01}	$3.0 \times 10^{+00}$	$5.35 \times 10^{+00}$

[1] H. Schatz and K. E. Rehm, Nucl. Phys. A **777**, 601 (2006).
[2] R. K. Wallace and S. E. Woosley, Astrophys. J. Suppl. Ser. **45**, 389 (21981).
[3] H. Schatz, A. Aprahamian, V. Barnard, L. Bildsten, A. Cumming, M. Ouellette, T. Rauscher, F.-K. Thielemann, and M. Wiescher, Nucl. Phys. A **688**, 150c (2001).
[4] J. L. Fisker, F.-K. Thielemann, and M. Wiescher, Astrophys. J. **608**, L61 (2004).
[5] A. Saastamoinen *et al.*, Phys. Rev. C **80**, 044330 (2009).
[6] H. Schatz *et al.*, Phys. Rev. Lett. **79**, 3845 (1997).
[7] H. Herndl, J. Görres, M. Wiescher, B. A. Brown, and L. V. Wormer, Phys. Rev. C **52**, 1078 (1995).
[8] A. Banu *et al.*, Phys. Rev. C **84**, 015803 (2011).
[9] L. Trache, F. Carstoiu, C. A. Gagliardi, R. E. Tribble, Phys. Rev. Lett. **87**, 271102 (2001); *id.*, Phys. Rev. C **69**, 032802(R)(2004).
[10] L. Bianchi *et al.*, Nucl. Instrum. Methods A **276**, 509 (1989).
[11] S. L. Shepherd *et al.*, Nucl. Instrum. Methods A **434**, 373 (1999).
[12] E. Sauvan *et al.*, Phys. Rev. C **69**, 044603 (2004).
[13] J. P. Jeukenne, A. Lejeune, and C. Mahaux, Phys. Rev. C **16**, 80 (1977).
[14] L. Trache, A. Azhari, H. L. Clark, C. A. Gagliardi, Y.-W. Lui, A. M. Mukhamedzhanov, and R. E. Tribble, Phys. Rev. C **61**, 024612 (2000).
[15] F. Carstoiu, R. E. Tribble, and C. A. Gagliardi, Phys. Rev. C **70**, 054610 (2004).
[16] E. D. Cooper, S. Hama, B. C. Clark, and R. L. Mercer, Phys. Rev. C **47**, 297 (1993).
[17] M. Beiner and R. J. Lombard, Ann. Phys. (N. Y.) **86**, 271102 (1974); F. Carstoiu and R. J. Lombard, *ibid.* **217**, 279 (1992).
[18] H. De Vries, C. W. De Jager, and C. De Vries, At. Data Nucl. Data Tables **36**, 495 (1987).
[19] H. M. Xu, C. A. Gagliardi, R. E. Tribble, A. M. Mukhamedzhanov, and N. K. Timofeyuk, Phys. Rev. Lett. **73**, 2027 (1994).
[20] B. A. Brown and W. A. Richter, Phys. Rev. C **74**, 034315 (2006).
[21] P. G. Hansen and J. A. Tostevin, Annu. Rev. Nucl. Part. Sci. **53**, 219 (2003).
[22] A. Gade *et al.*, Phys. Rev. C **77**, 044306 (2008).
[23] C. A. Bertulani, Comput. Phys. Commun. **156**, 123 (2003).
[24] W. A. Fowler, G. R. Caughlan, and B. A. Zimmermann, Annu. Rev. Astro. Astrophys. **5**, 525 (1967).
[25] W. A. Fowler, G. R. Caughlan, and B. A. Zimmermann, Annu. Rev. Astro. Astrophys. **13**, 69 (1975).
[26] C. Iliadis, J. M. D'Auria, S. Starrfield, W. J. Thompson, and M. Wiescher, Astrophys. J. Suppl. Ser. **134**, 151 (2001).
[27] A. Parikh, J. Jose, F. Moreno, and C. Iliadis, Astrophys. J. Suppl. Ser. **178**, 110 (2008).